

Supporting Information  
for DOI: 10.1055/s-0035-1560088  
© Georg Thieme Verlag KG Stuttgart · New York 2015

## Supporting Information

### Racemization-Free Synthesis of Morpholinone Derivatives from $\alpha$ -Amino Acids

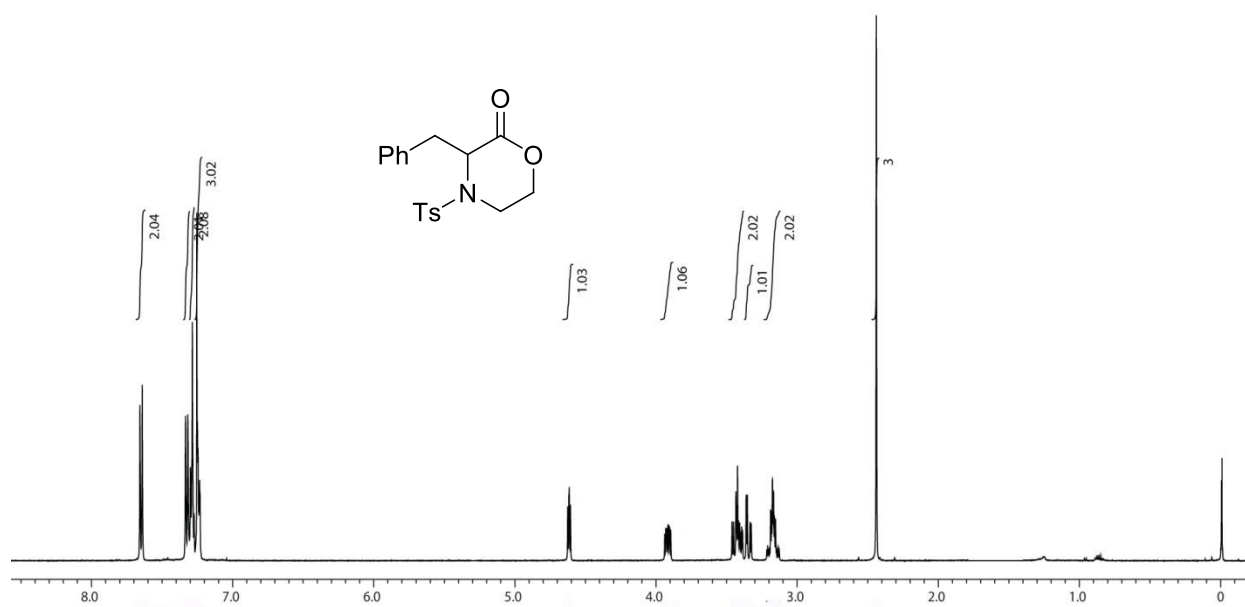
Sauvik Samanta, Abhijit Mal, Sandipan Halder and Manas K. Ghorai\*

SL No	Contents	Page No
1	General Information	2
2	Selected NMR spectra	3
3	Selected HPLC chromatograms for <i>ee</i> determination	20
4	X-ray crystal structures	23
5	X-ray crystallographic analysis of <b>2a</b> and <b>2b</b>	23
6	References	24

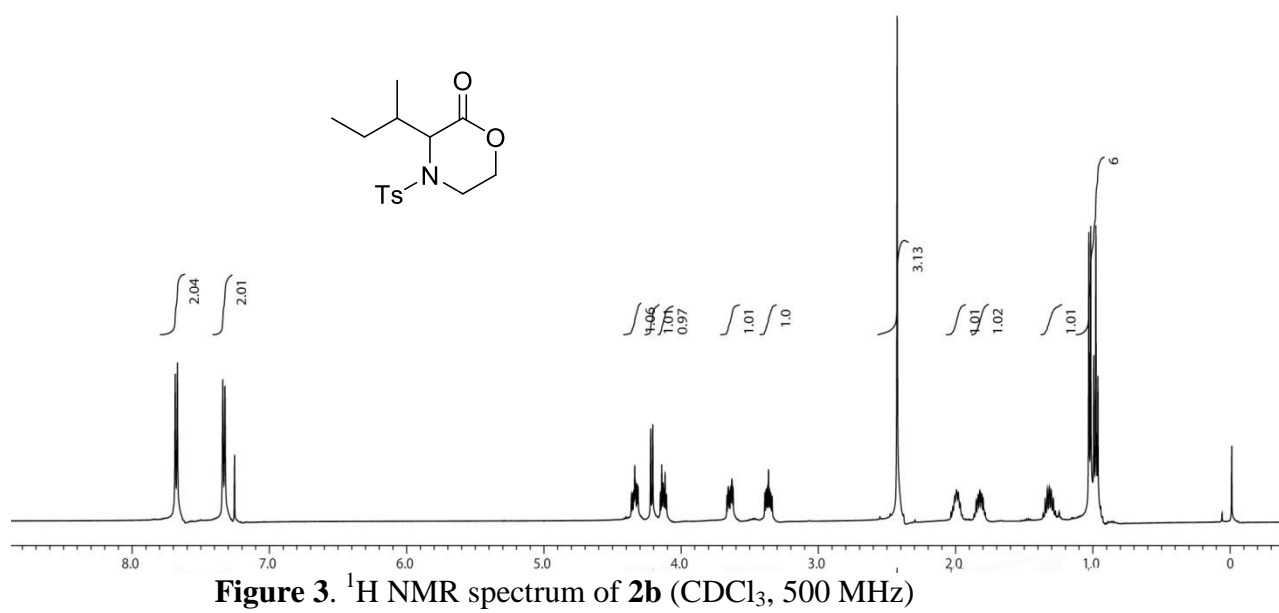
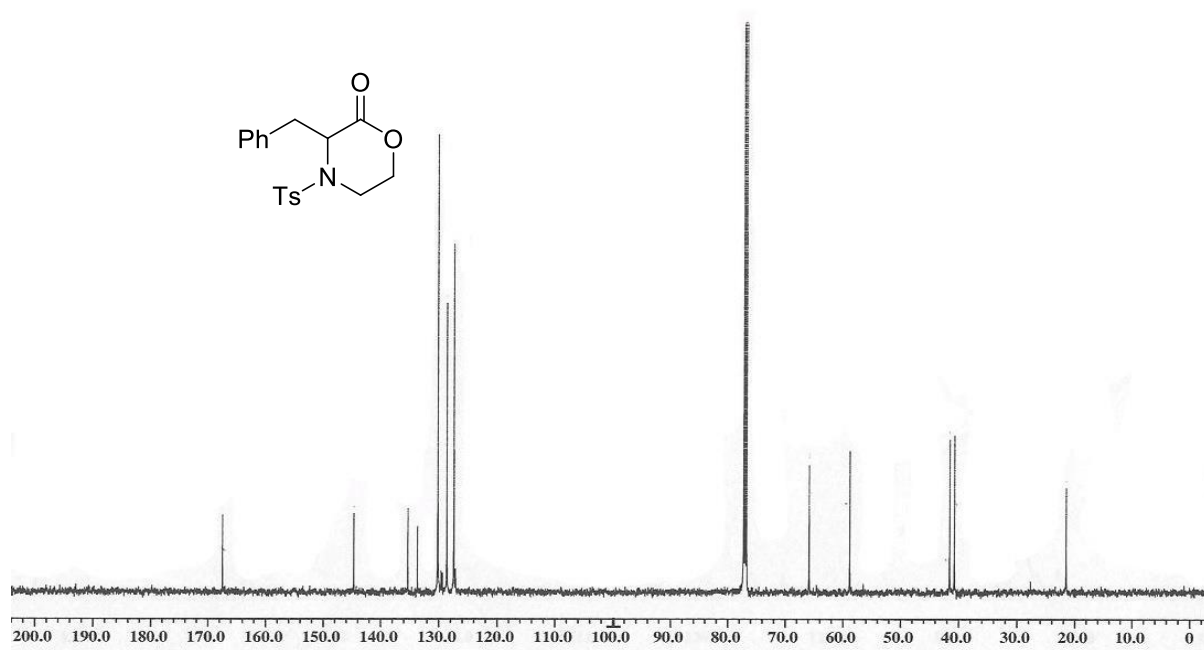
## 1. General Information

Analytical thin layer chromatography (TLC) was carried out using silica gel 60 F<sub>254</sub> pre-coated plates. Visualization was accomplished with UV lamp or I<sub>2</sub> stain. Silica gel 230–400 mesh size was used for flash column chromatography using the combination of ethyl acetate and petroleum ether as eluent. Unless noted, all reactions were carried out in oven-dried glassware under an atmosphere of nitrogen/argon using anhydrous solvents. Where appropriate, all reagents were purified prior to use following the guidelines of Perrin and Armarego.<sup>1</sup> All commercial reagents were used as received. Proton nuclear magnetic resonance (<sup>1</sup>H NMR) spectra were recorded at 400 MHz/500 MHz. Chemical shifts were recorded in parts per million (ppm,  $\delta$ ) relative to tetramethyl silane ( $\delta$  0.00). <sup>1</sup>H NMR splitting patterns are designated as singlet (s), doublet (d), doublet of doublet (dd), triplet (t), quartet (q), multiplet (m). Carbon nuclear magnetic resonance (<sup>13</sup>C NMR) spectra were recorded at 100 MHz/125 MHz. Mass spectra (MS) were obtained using ESI mass spectrometers. IR spectra were recorded as neat for liquid and in KBr for solids. Melting points were determined using a hot stage apparatus and were uncorrected. Optical rotations were measured using a 2.0 mL cell with a 1.0 dm path length and are reported as  $[\alpha]_D^{25}$  (*c* in g per 100 mL, solvent) at 25 °C. Enantiomeric excess (*ee*) was determined by HPLC using chiralcel AD-H, OD-H or AS-H analytical column (detection at 254 nm).

## 2. Selected NMR Spectra



**Figure 1.**  $^1\text{H}$  NMR spectrum of **2a** ( $\text{CDCl}_3$ , 500 MHz)



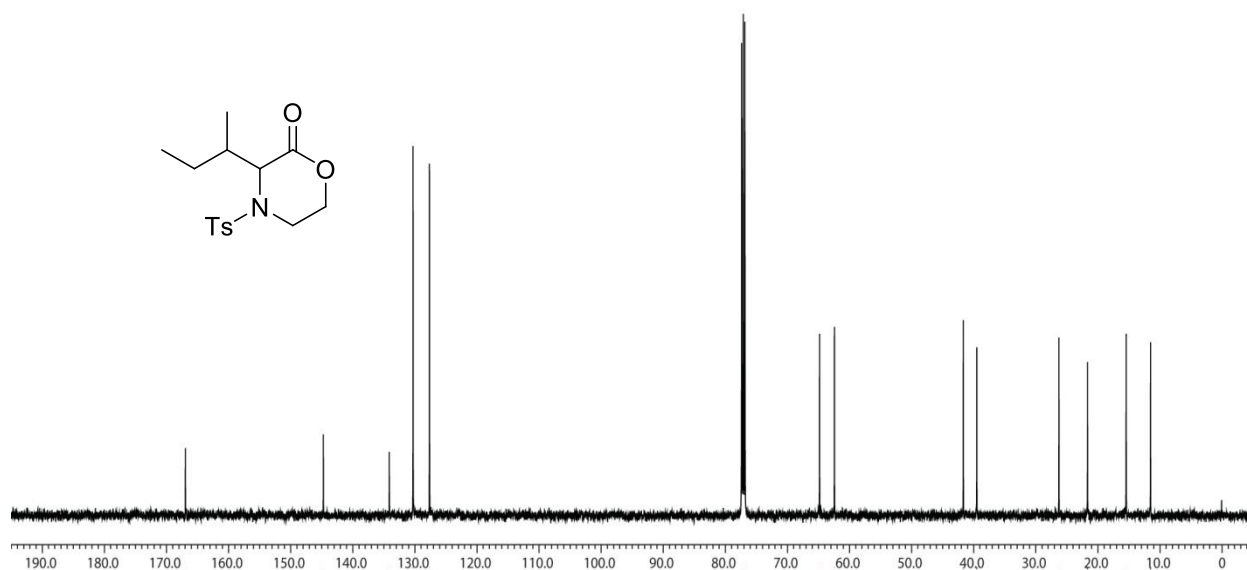


**Figure 4.**  $^{13}\text{C}$  NMR spectrum of **2b** ( $\text{CDCl}_3$ , 125 MHz)

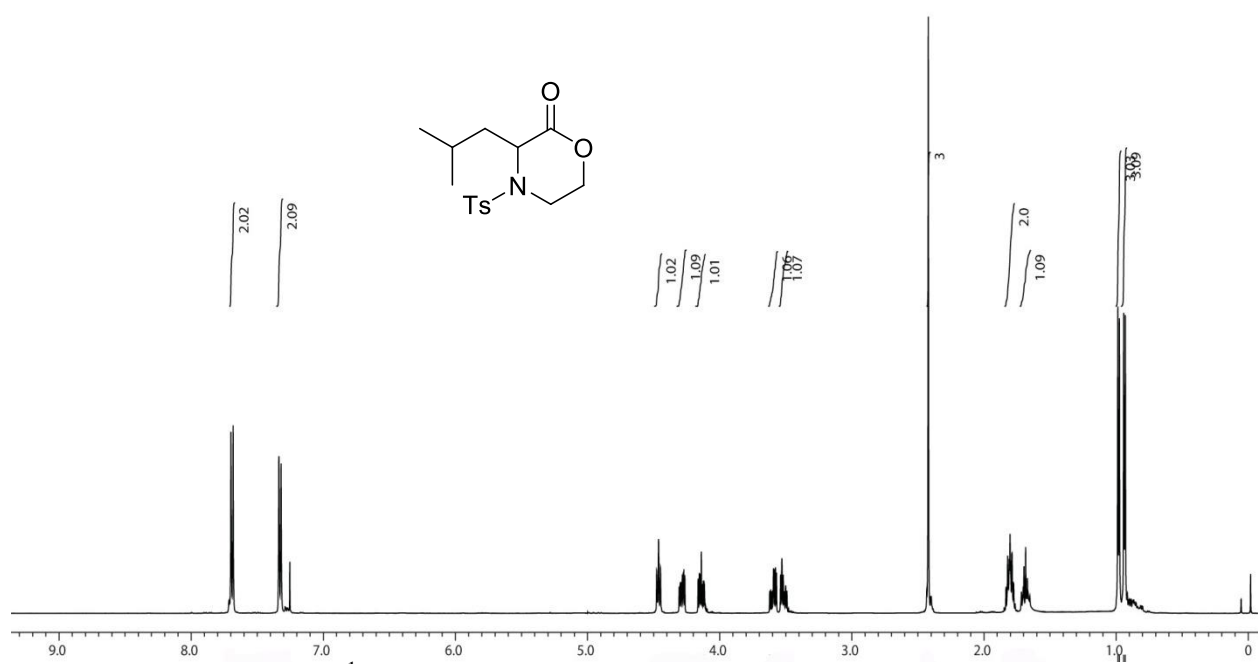


**Figure 5.**  $^1\text{H}$  NMR spectrum of **2c** ( $\text{CDCl}_3$ , 500 MHz)

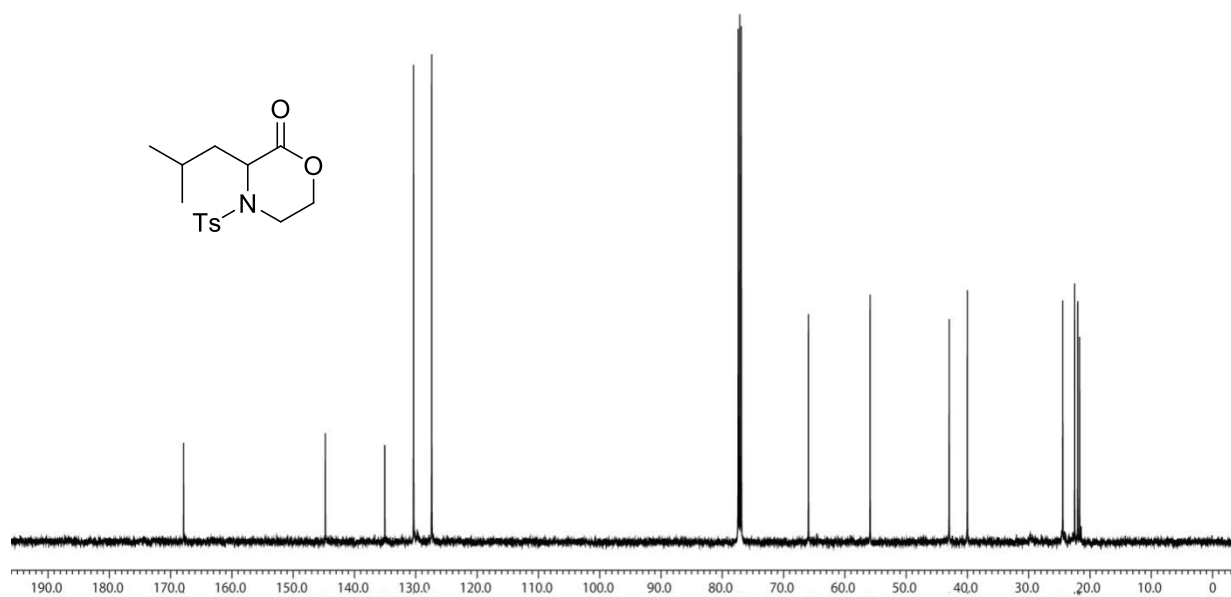


**Figure 6.**  $^{13}\text{C}$  NMR spectrum of **2c** ( $\text{CDCl}_3$ , 125 MHz)

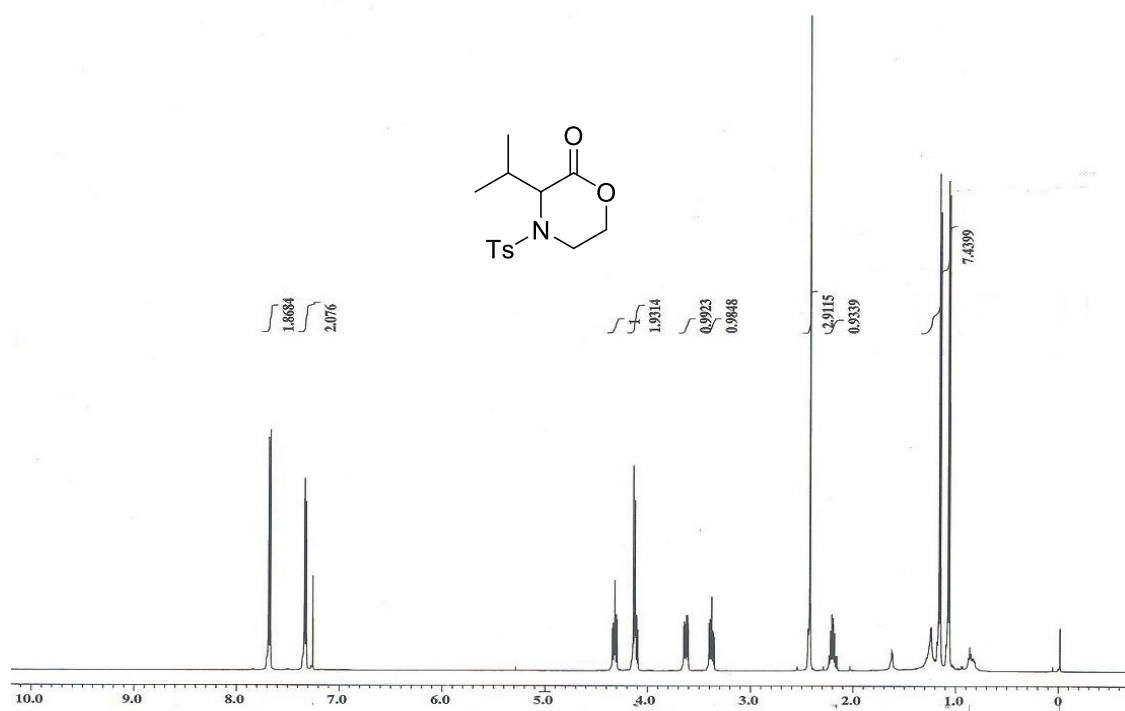


**Figure 7.**  $^1\text{H}$  NMR spectrum of **2d** ( $\text{CDCl}_3$ , 500 MHz)

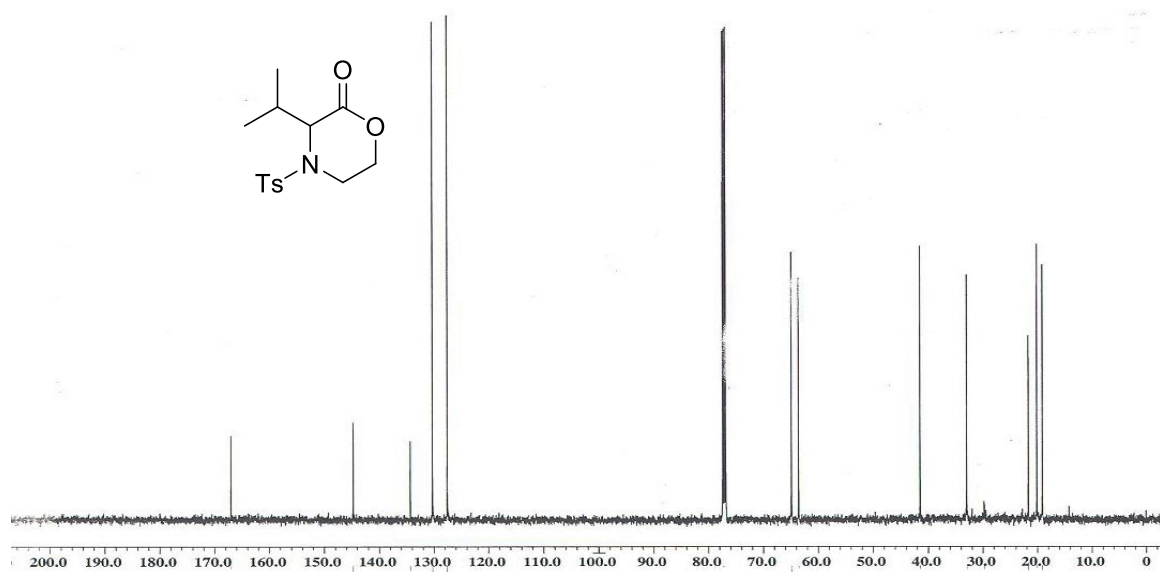


**Figure 8.**  $^{13}\text{C}$  NMR spectrum of **2d** ( $\text{CDCl}_3$ , 125 MHz)

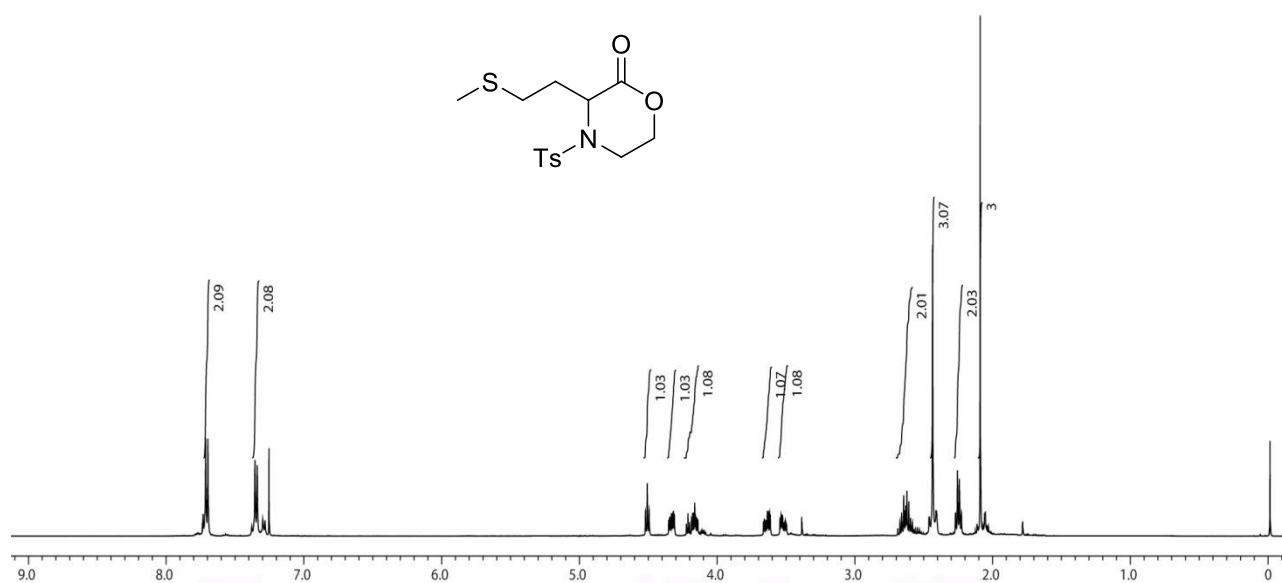


**Figure 9.**  $^1\text{H}$  NMR spectrum of **2e** ( $\text{CDCl}_3$ , 500 MHz)

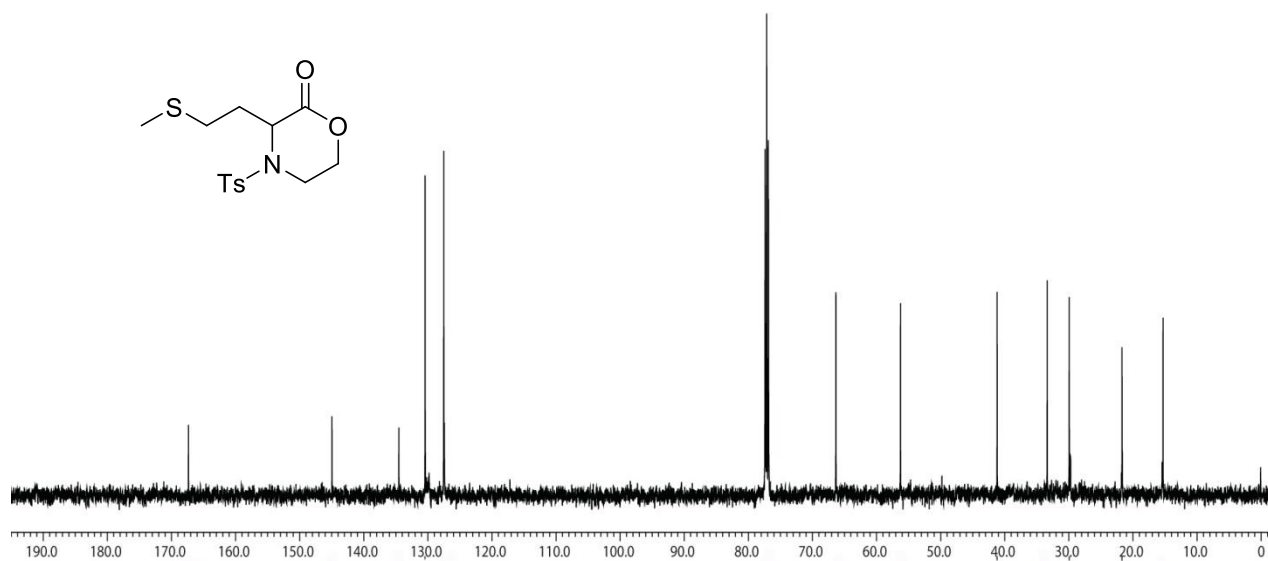


**Figure 10.**  $^{13}\text{C}$  NMR spectrum of **2e** ( $\text{CDCl}_3$ , 125 MHz)

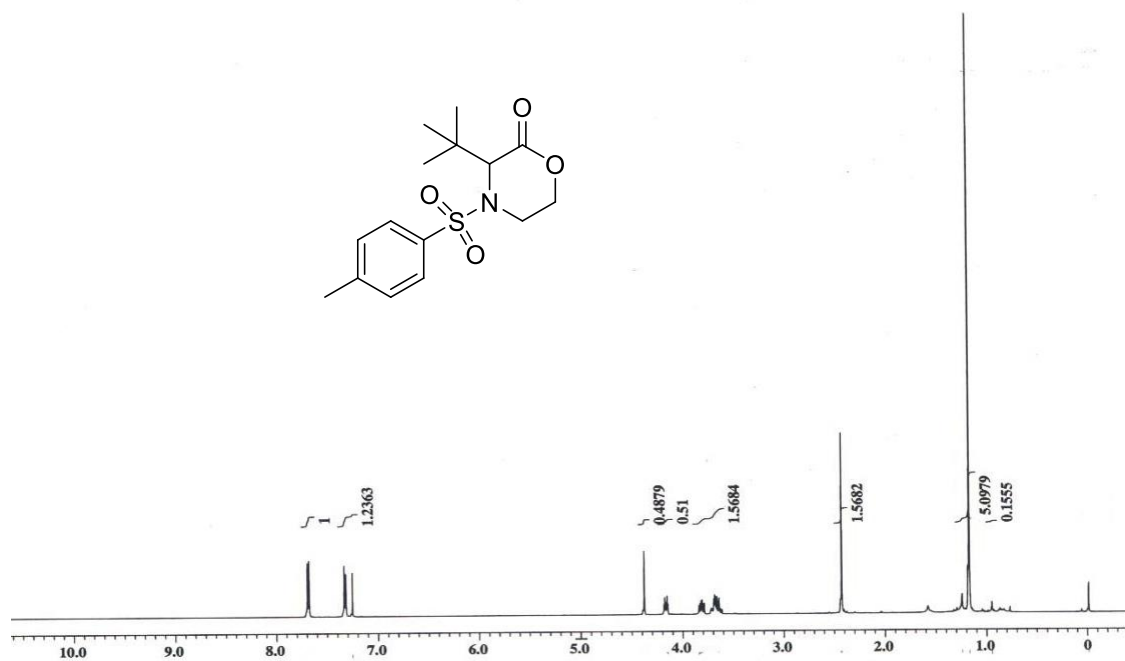


**Figure 11.**  $^1\text{H}$  NMR spectrum of **2f** ( $\text{CDCl}_3$ , 500 MHz)

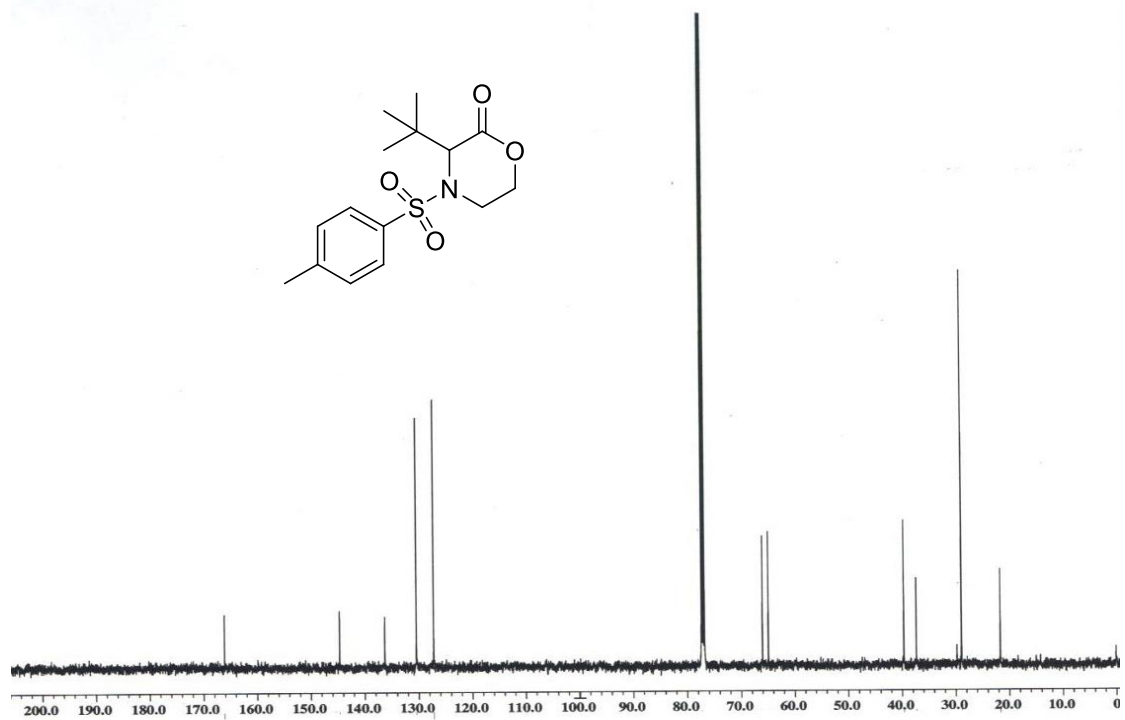
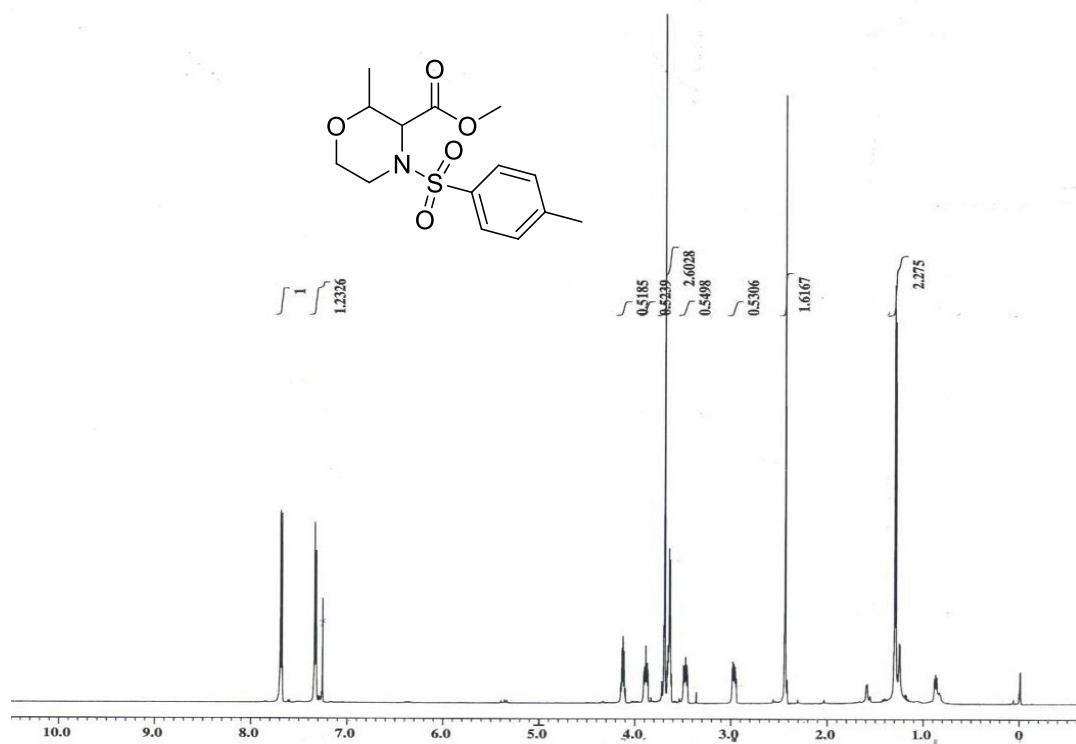
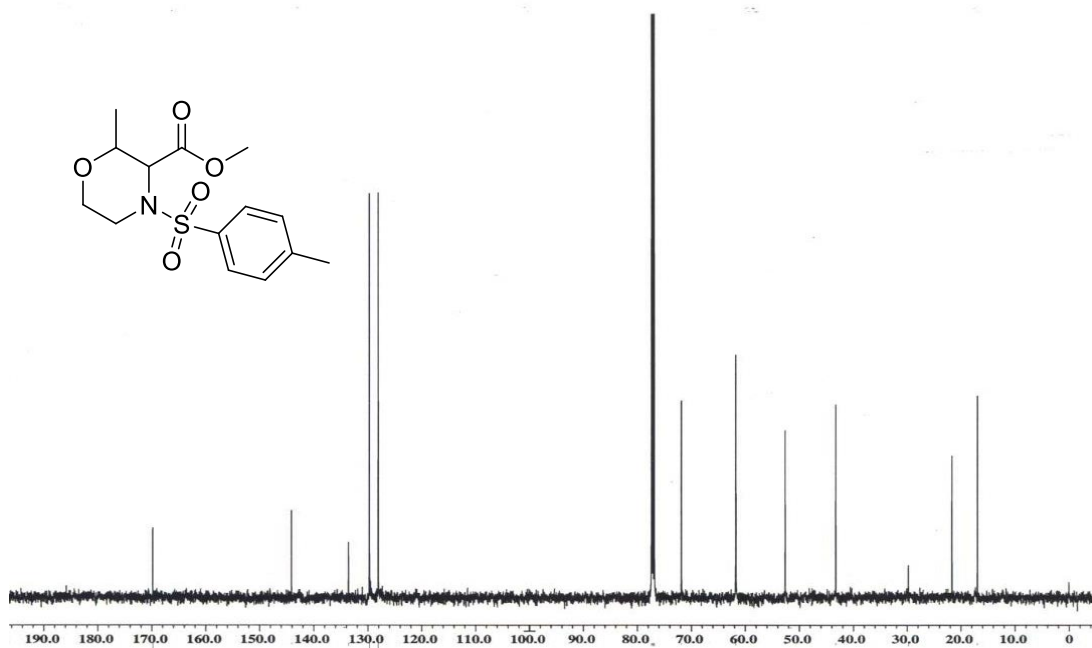


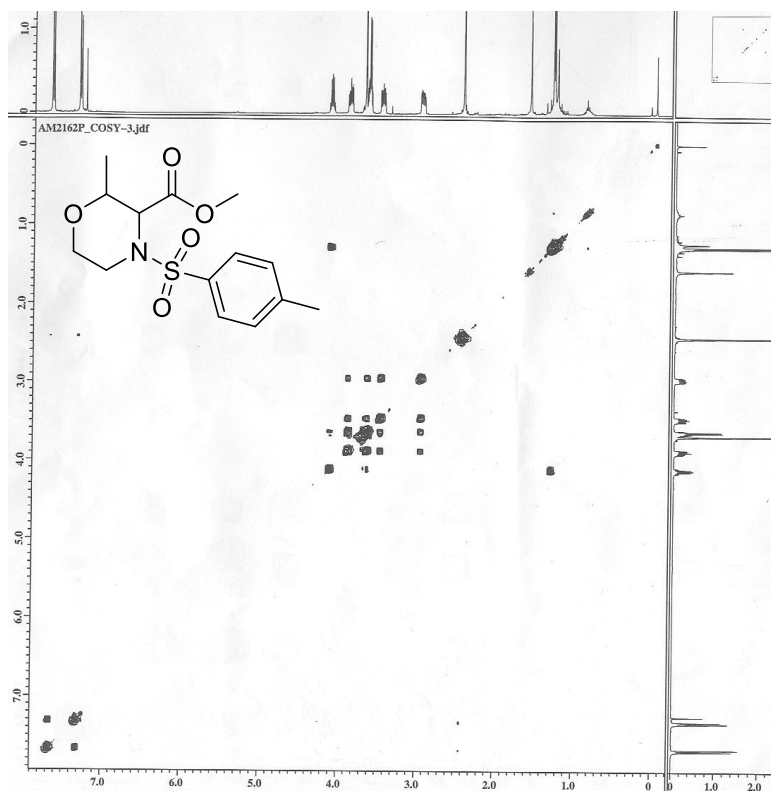
Figure 12.  $^{13}\text{C}$  NMR spectrum of **2f** ( $\text{CDCl}_3$ , 125 MHz)



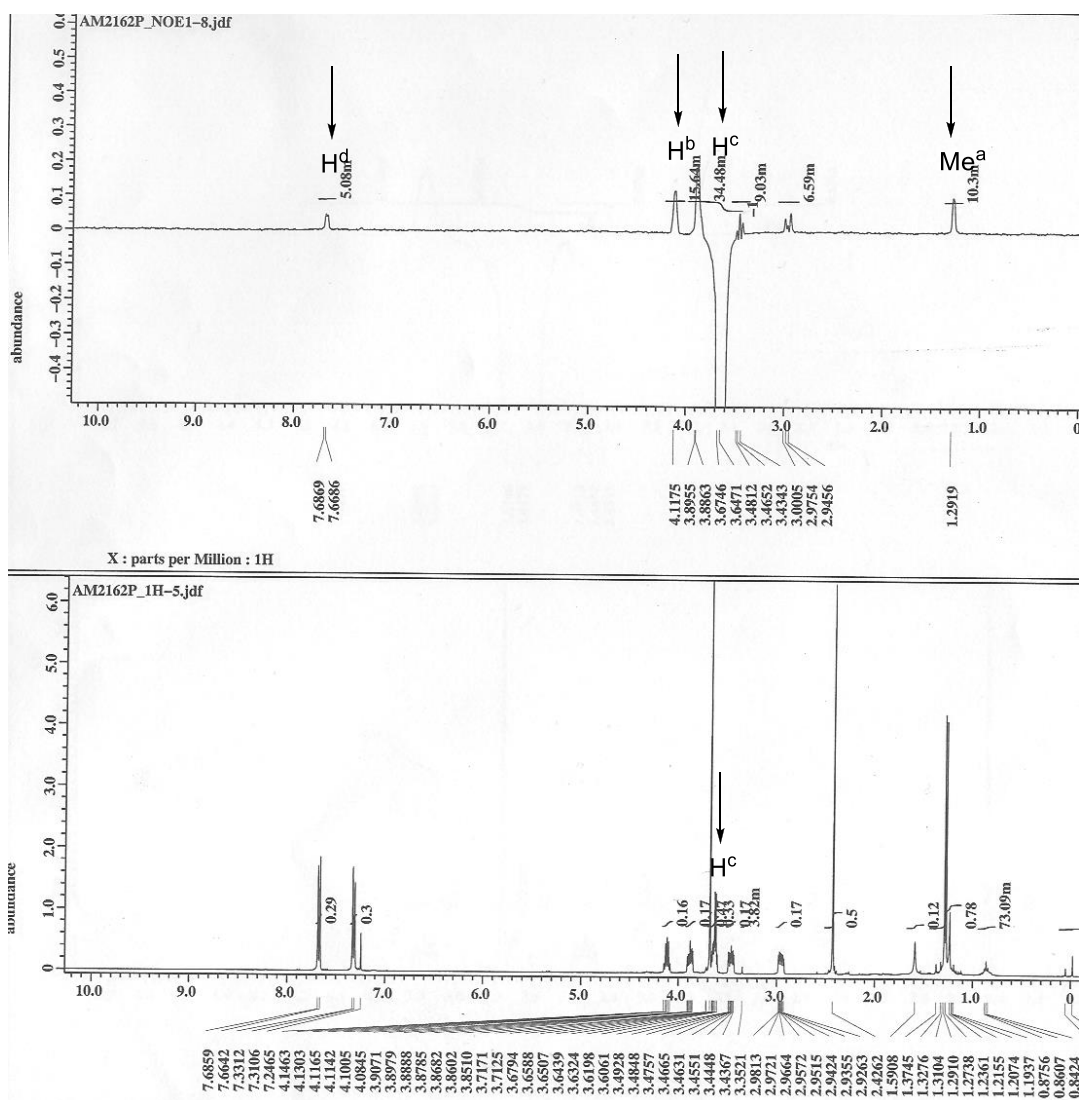
**Figure 13.**  $^1\text{H}$  NMR spectrum **7** ( $\text{CDCl}_3$ , 500 MHz)



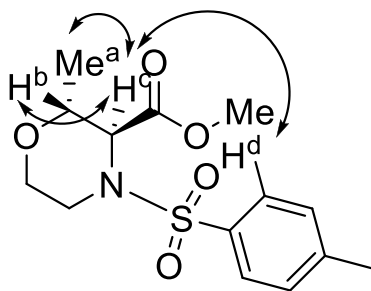
**Figure 14.**  $^{13}\text{C}$  NMR spectrum **7** ( $\text{CDCl}_3$ , 125 MHz)

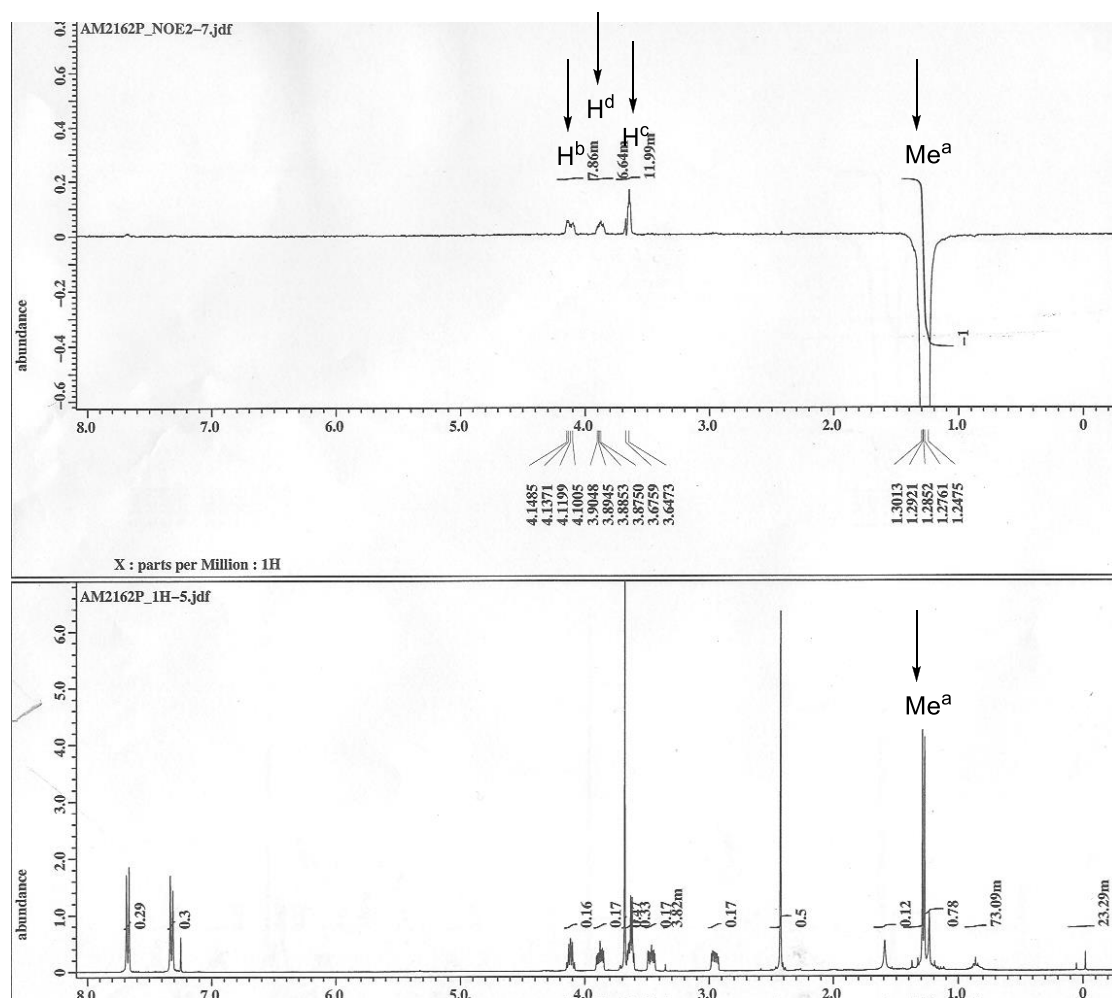


**Figure 15.**  $^1\text{H}$ - $^1\text{H}$  COSY spectrum of **7** ( $\text{CDCl}_3$ , 400 MHz)

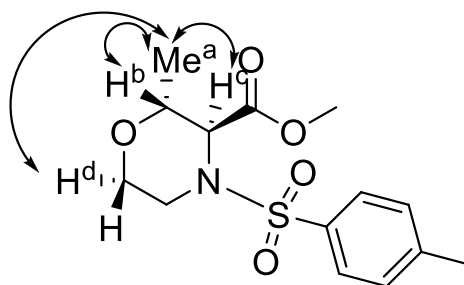


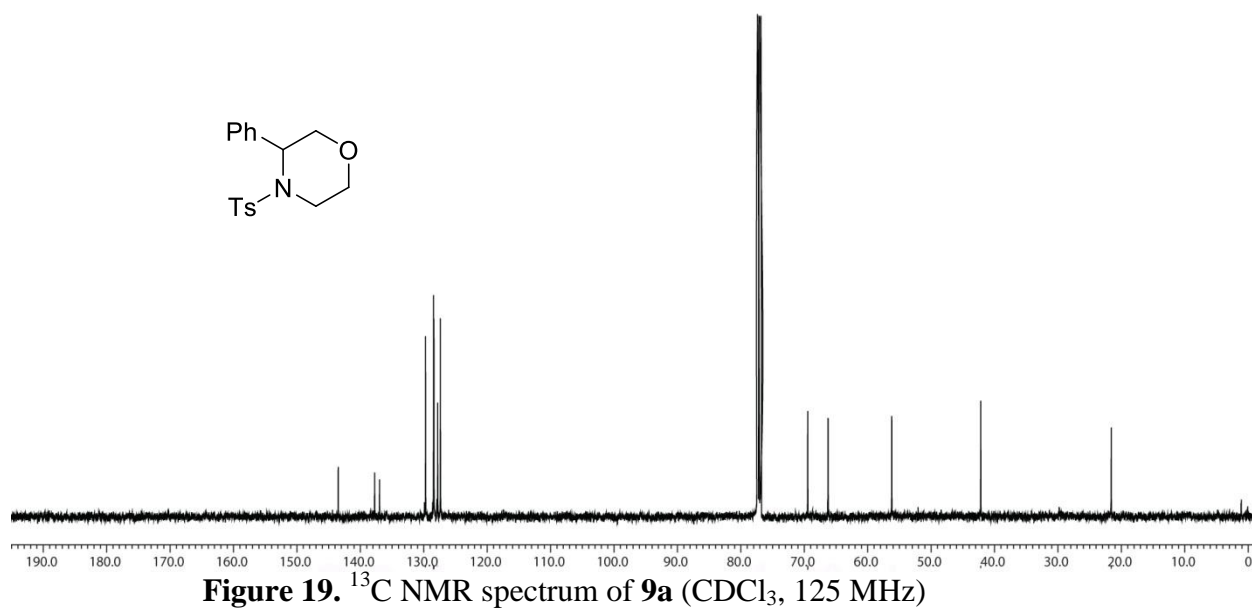
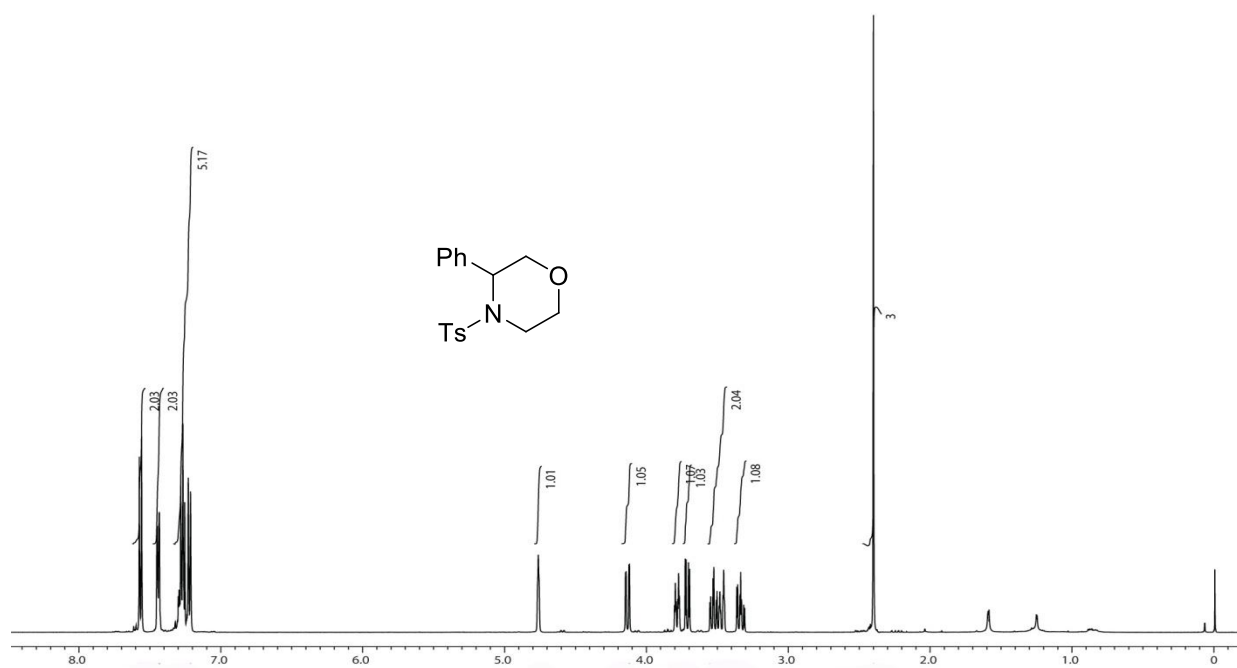
**Figure 16.**  $^1\text{H}$  nOe spectrum of **7** showing correlation between  $\text{H}^c$ - $\text{Me}^a$ ,  $\text{H}^c$ - $\text{H}^b$  and  $\text{H}^c$ - $\text{H}^d$  (when  $\text{H}^c$  is irradiated, intensities of  $\text{Me}^a$ ,  $\text{H}^b$  and  $\text{H}^d$  are enhanced) ( $\text{CDCl}_3$ , 400 MHz)





**Figure 17.**  $^1\text{H}$  nOe spectrum of **7** showing correlation between  $\text{Me}^a$ - $\text{H}^b$ ,  $\text{Me}^a$ - $\text{H}^c$  and  $\text{Me}^a$ - $\text{H}^d$  (when  $\text{Me}^a$  is irradiated, intensities of  $\text{H}^b$ ,  $\text{H}^c$  and  $\text{H}^d$  are enhanced) ( $\text{CDCl}_3$ , 400 MHz)





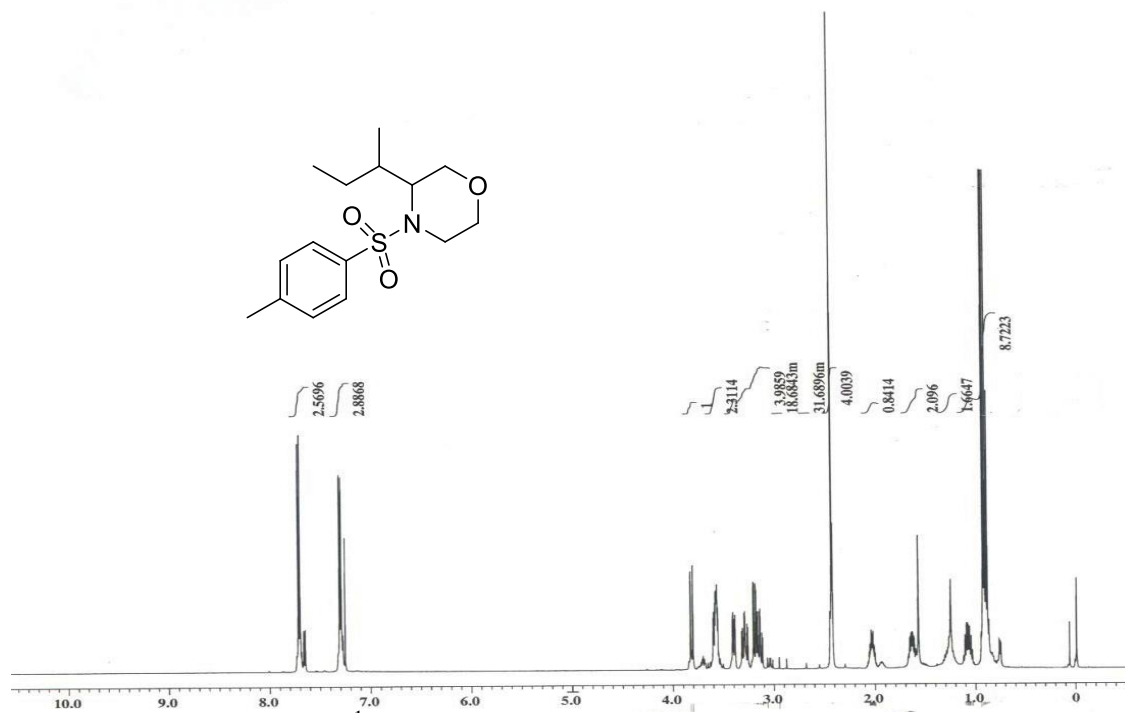


**Figure 20.**  $^1\text{H}$  NMR spectrum of **9b** ( $\text{CDCl}_3$ , 500 MHz)

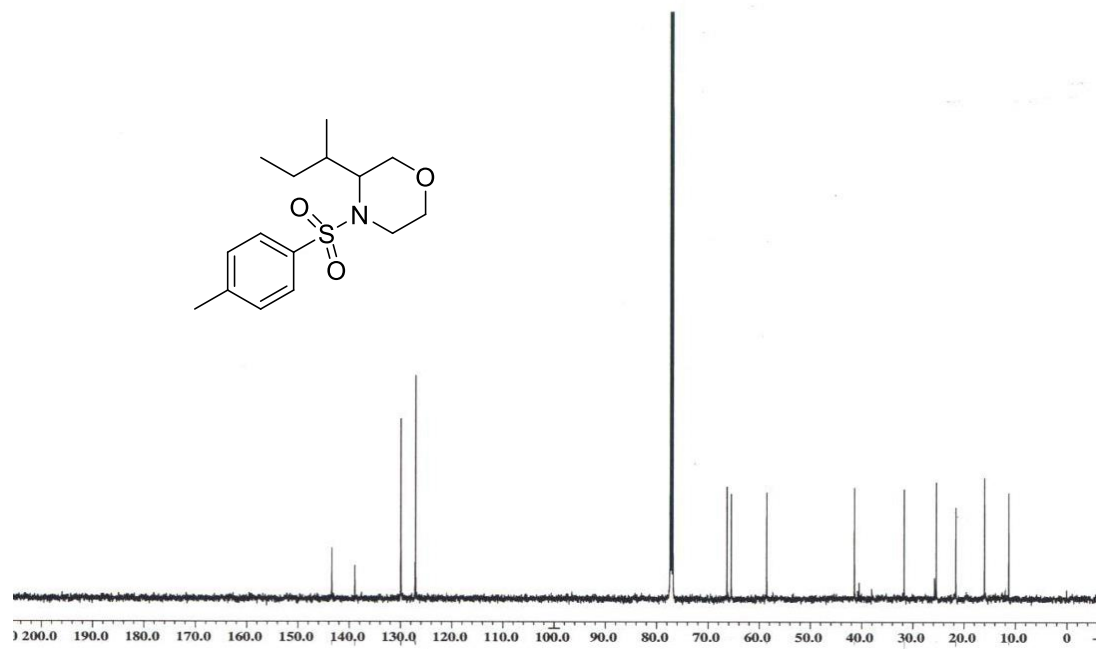


**Figure 21.**  $^{13}\text{C}$  NMR spectrum of **9b** ( $\text{CDCl}_3$ , 125 MHz)

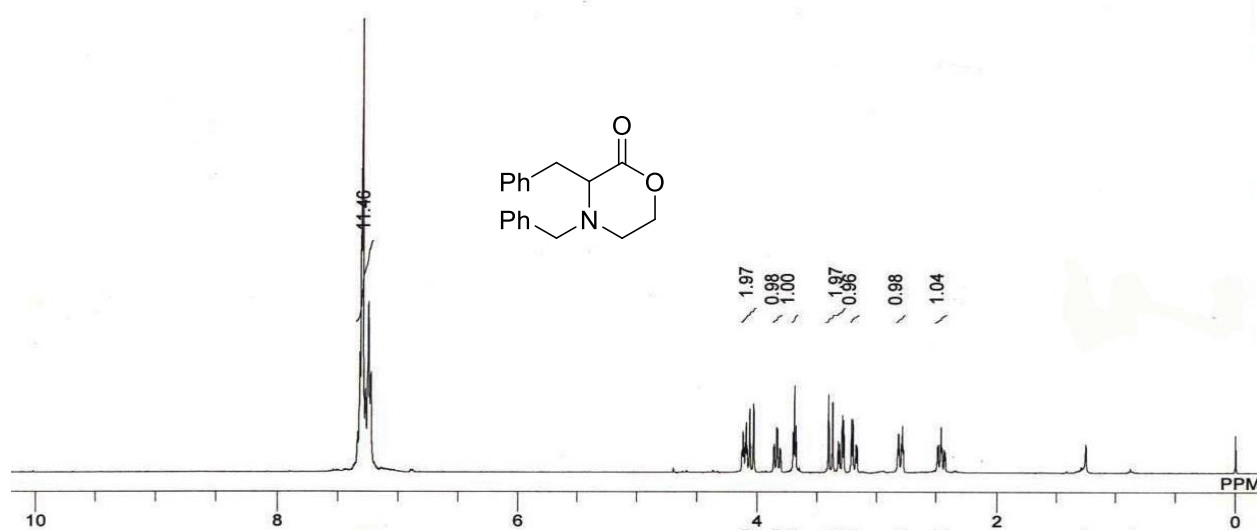


Figure 22.  $^1\text{H}$  NMR spectrum of **11a** ( $\text{CDCl}_3$ , 400 MHz)

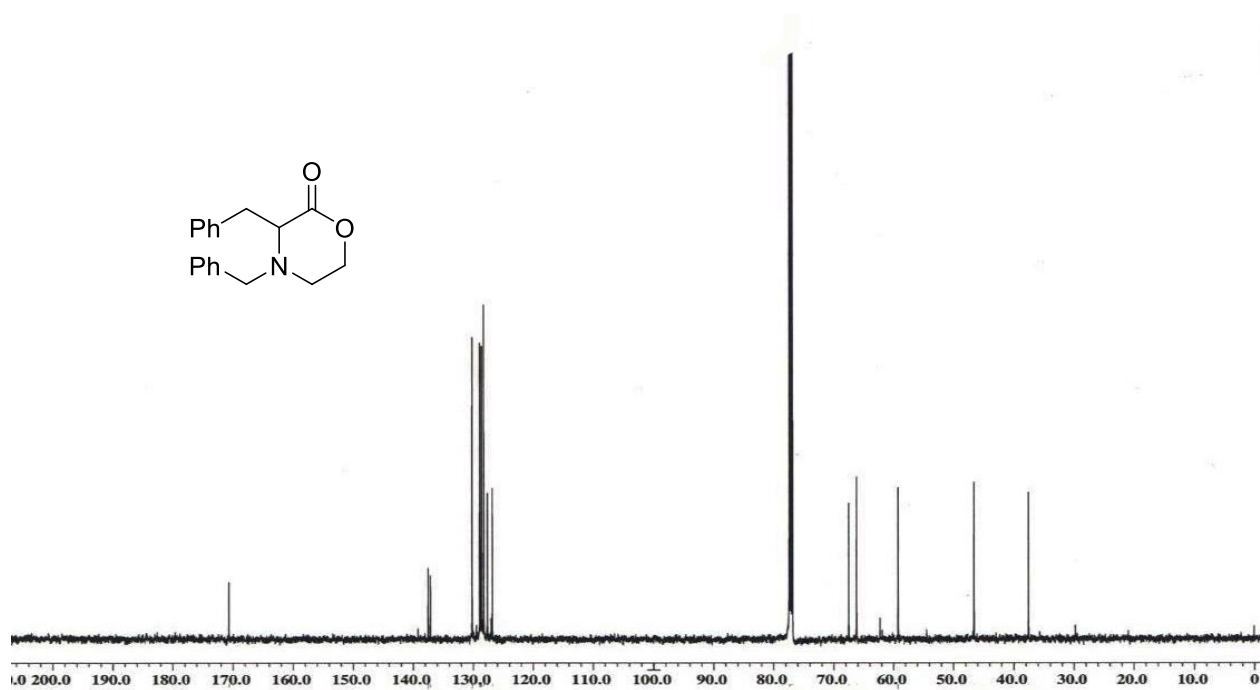
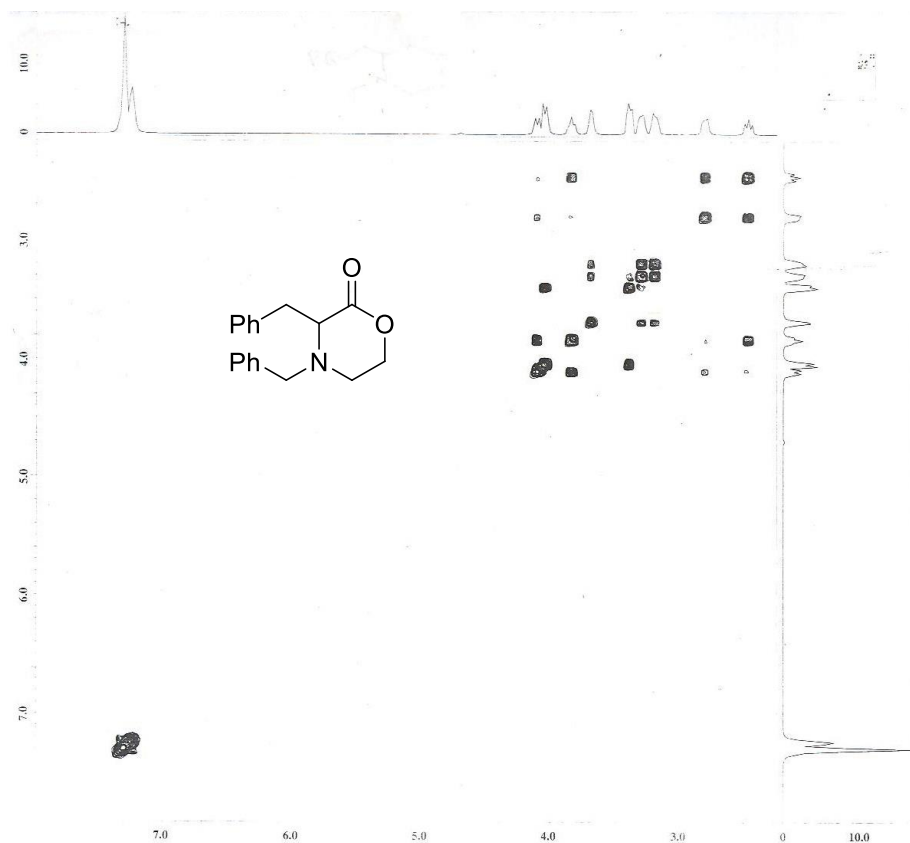
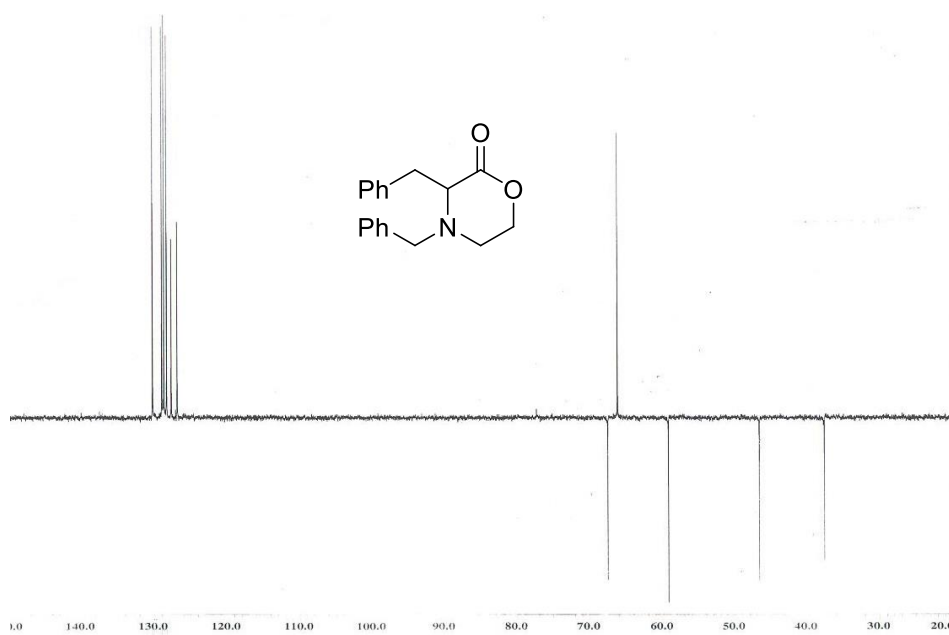


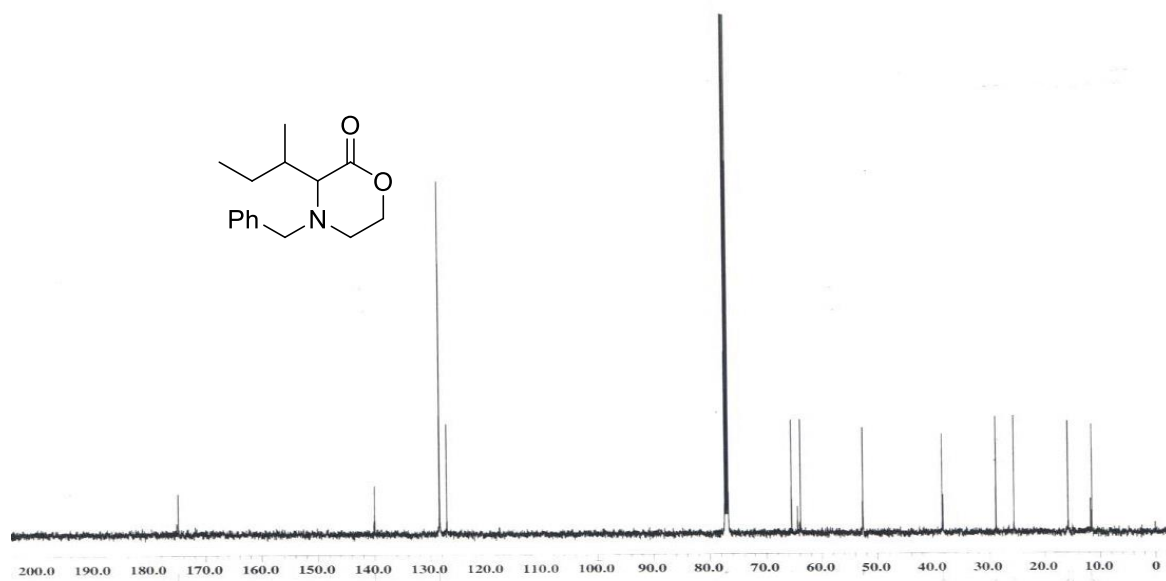
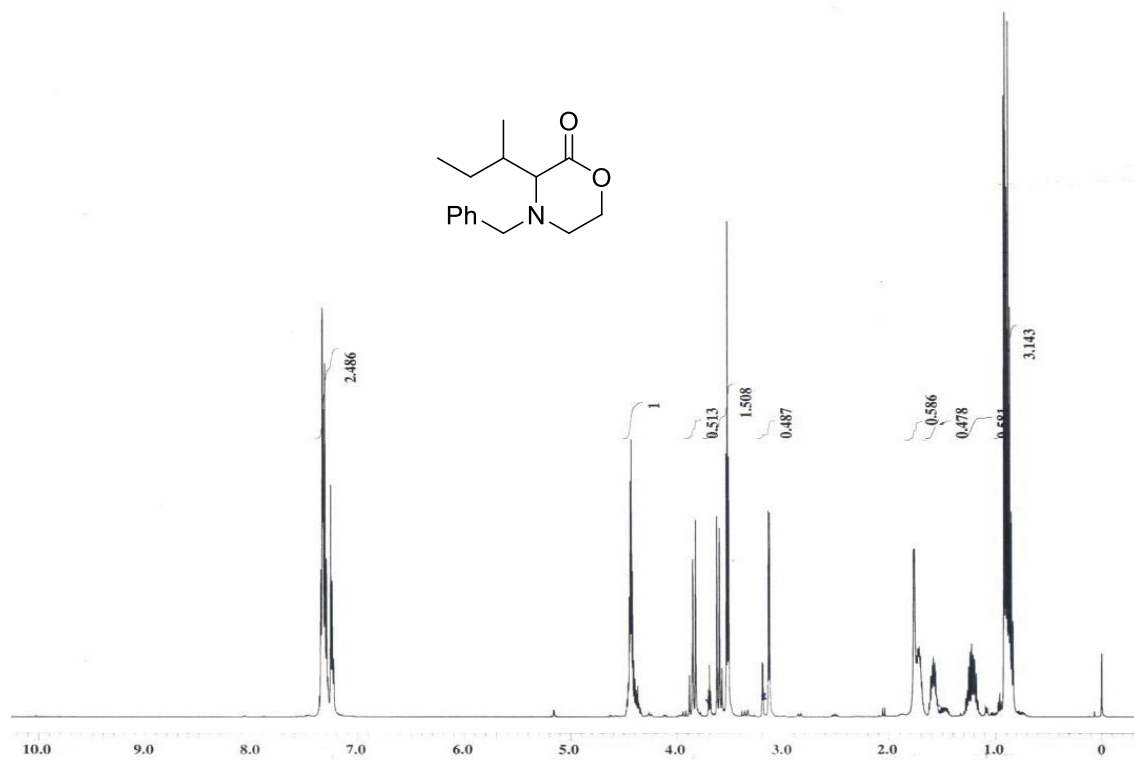
Figure 23.  $^{13}\text{C}$  NMR spectrum of **11a** ( $\text{CDCl}_3$ , 100 MHz)



**Figure 24.**  $^1\text{H}$ - $^1\text{H}$  COSY spectrum of **11a** ( $\text{CDCl}_3$ , 500 MHz)



**Figure 25.** DEPT 135 spectrum of **11a** ( $\text{CDCl}_3$ , 125 MHz)



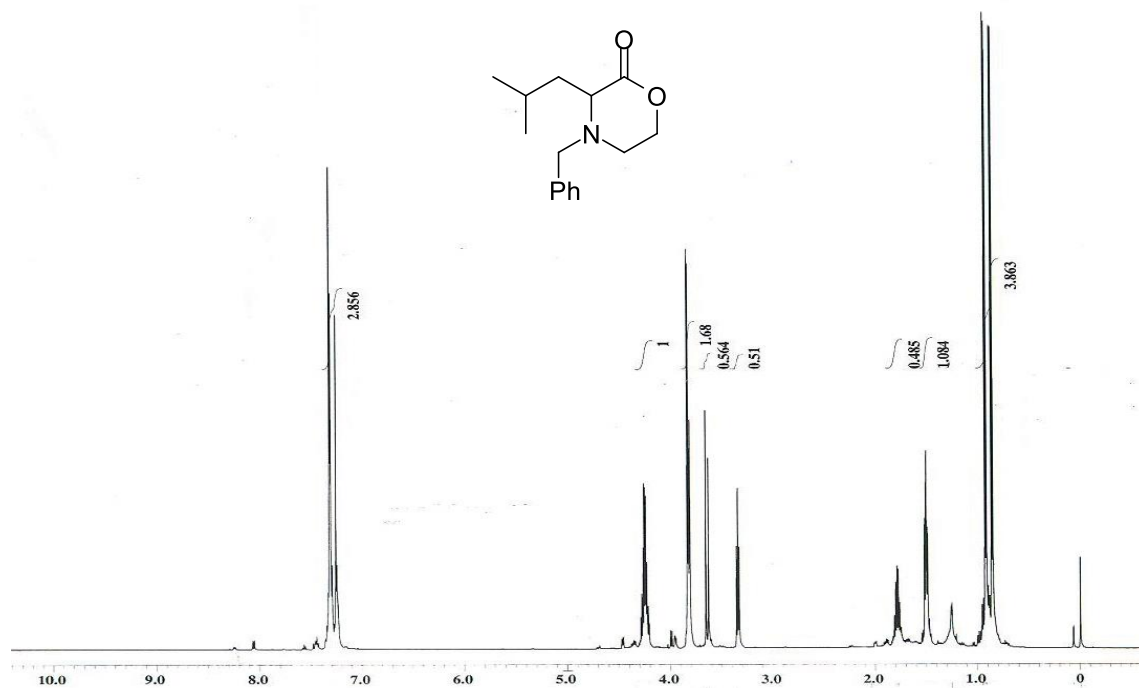


**Figure 28.**  $^1\text{H}$  NMR spectrum of **11c** ( $\text{CDCl}_3$ , 500 MHz)

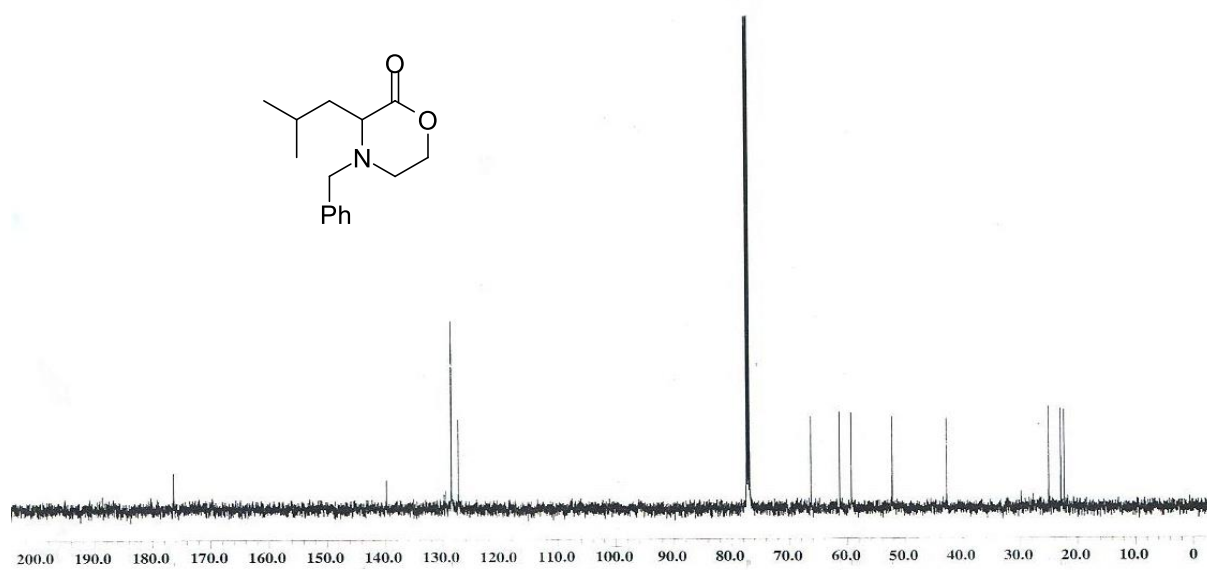


**Figure 29.**  $^{13}\text{C}$  NMR spectrum of **11c** ( $\text{CDCl}_3$ , 125 MHz)

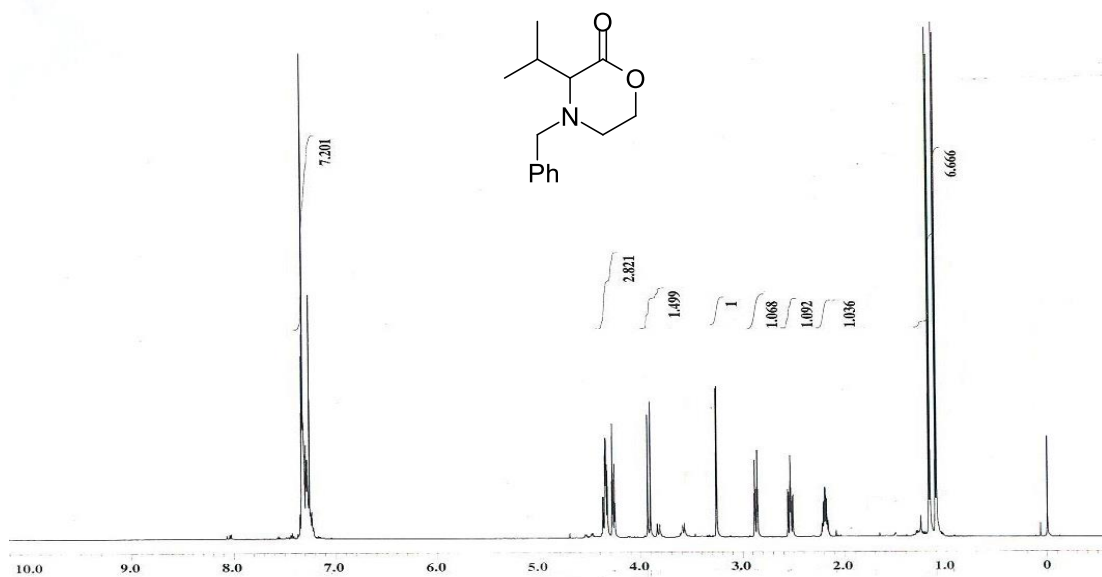


**Figure 30.** <sup>1</sup>H NMR spectrum of **11d** (CDCl<sub>3</sub>, 500 MHz)

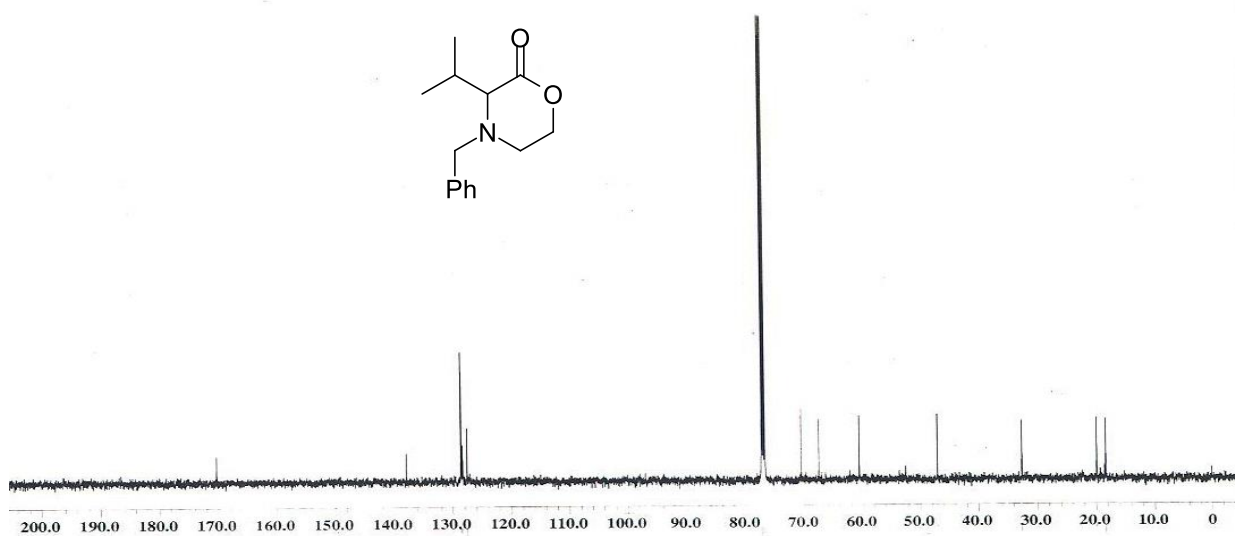


**Figure 31.** <sup>13</sup>C NMR spectrum of **11d** (CDCl<sub>3</sub>, 125 MHz)

### 3. Selected HPLC chromatograms for *ee* determination:

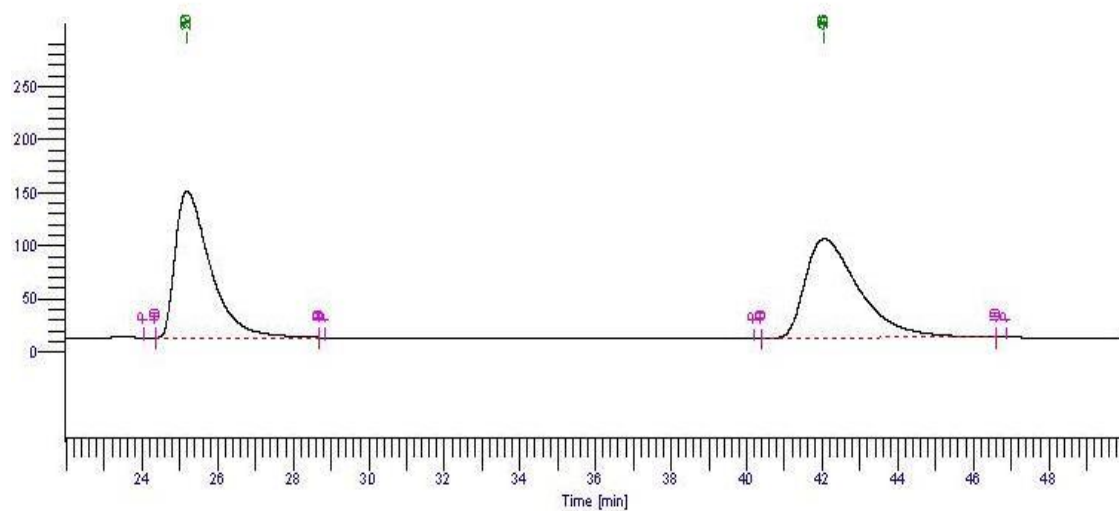


**Figure 32.** HPLC chromatogram of racemic compound **2b** (Cellulose 2 column; 90:10 Hexane–Isopropanol; 1.0 mL min<sup>-1</sup>)

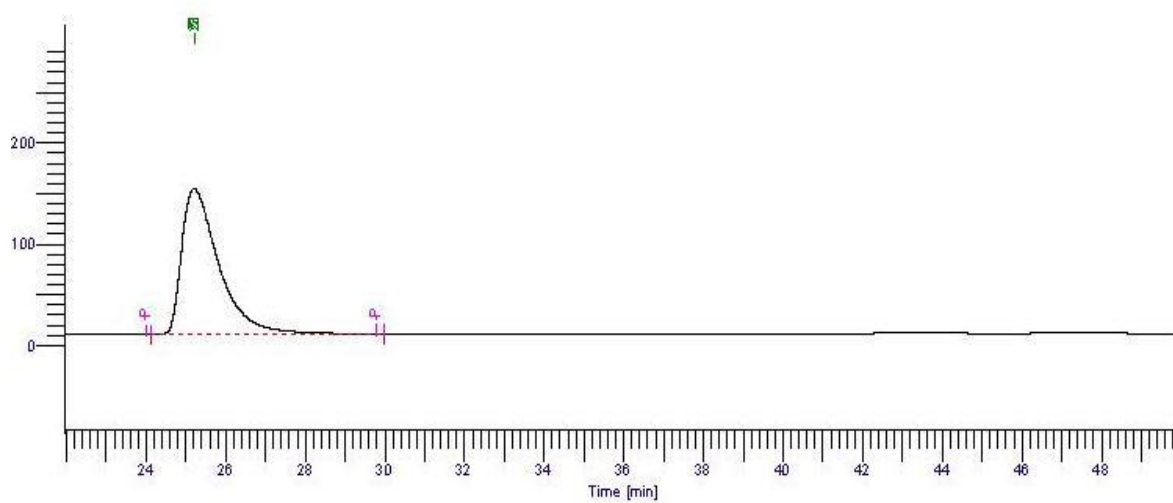


**Figure 33.** HPLC chromatogram of chiral compound **2b** (>99% *ee*; Cellulose 2 column; 90:10 Hexane–Isopropanol; 1.0 mL min<sup>-1</sup>)

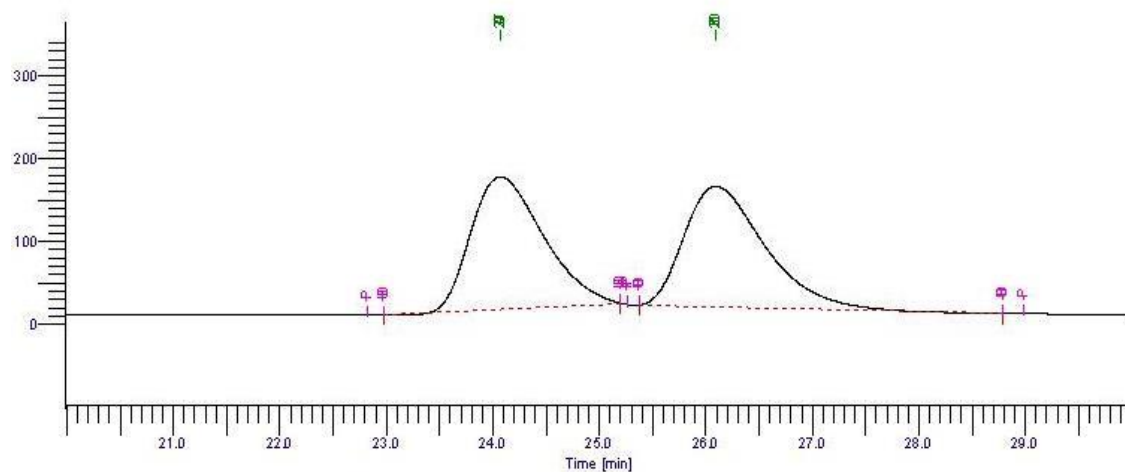


**Figure 34.** HPLC chromatogram of racemic compound **9a** (Cellulose 2 column; 90:10 Hexane–Isopropanol; 1.0 mL min<sup>-1</sup>)

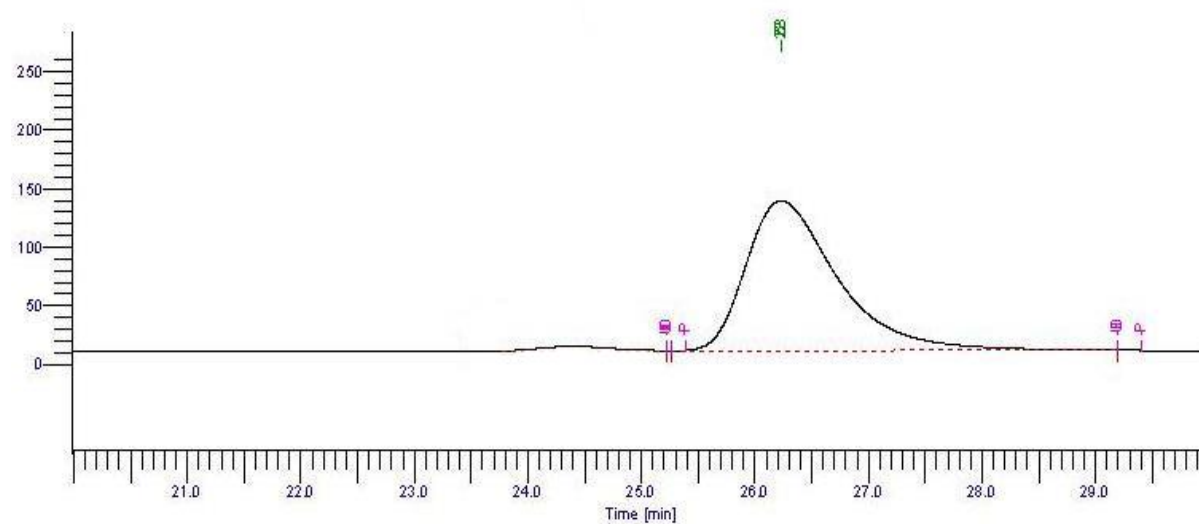


**Figure 35.** HPLC chromatogram of chiral compound **9a** (>99% *ee*; Cellulose 2 column; 90:10 Hexane–Isopropanol; 1.0 mL min<sup>-1</sup>)

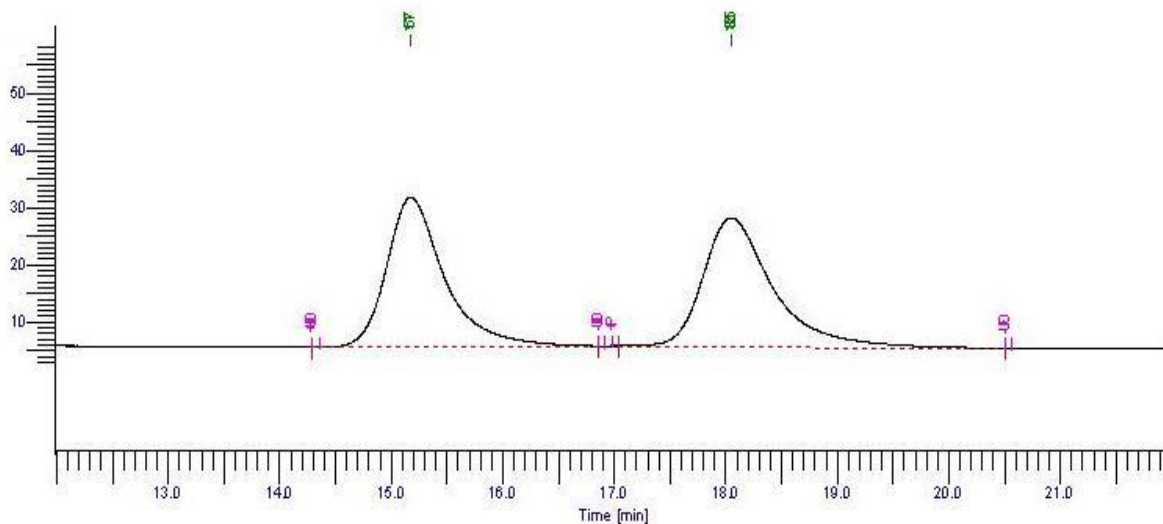


**Figure 36.** HPLC chromatogram of racemic compound **11a** (Cellulose 2 column; 90:10 Hexane–Isopropanol; 1.0 mL min<sup>-1</sup>)

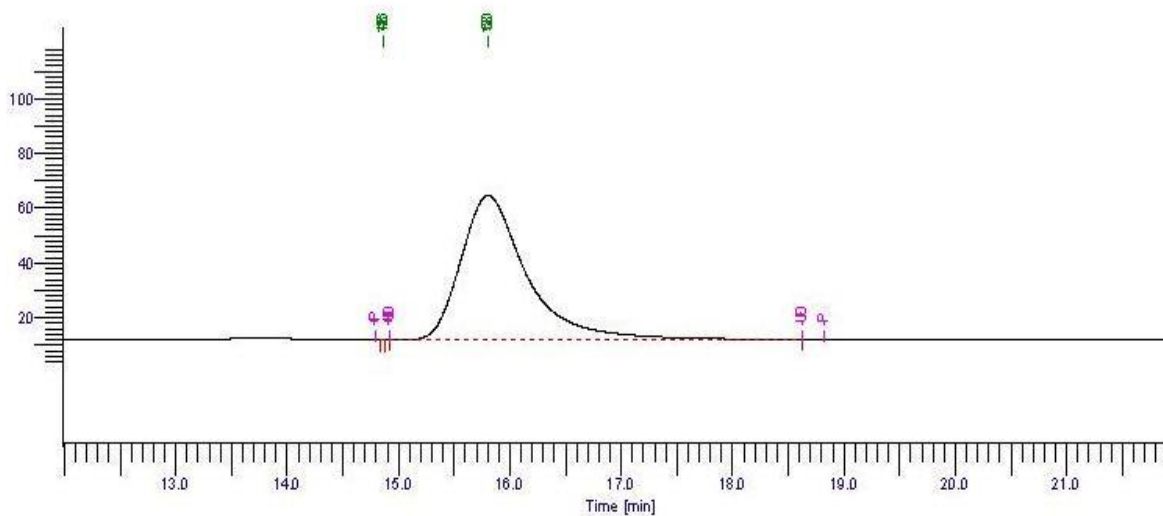


**Figure 37.** HPLC chromatogram of chiral compound **11a** (>99% *ee*; Cellulose 2 column; 90:10 Hexane–Isopropanol; 1.0 mL min<sup>-1</sup>)

#### 4. X-ray crystal structures:

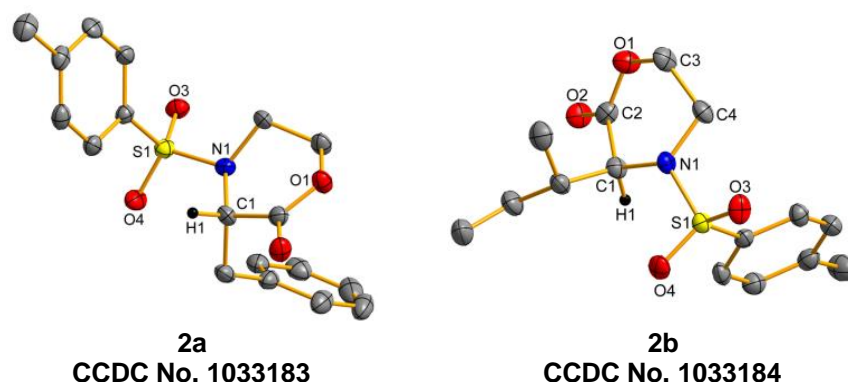


**Figure 38.** X-ray crystal structure of **2a** and **2b**

#### 5. X-ray crystallographic analysis of **2a** and **2b**:

The crystals used in the analyses were glued to a glass fiber and mounted on SMART APEX diffractometer. The instrument was equipped with CCD area detector and data were collected using graphite-monochromated Mo K $\alpha$  radiation ( $\lambda = 0.71069 \text{ \AA}$ ) at low temperature (100K). Cell constants were obtained from the least-squares refinement of three-dimensional centroids through the use of CCD recording of narrow  $\omega$  rotation frames, completing almost all-reciprocal space in the stated  $\theta$  range. All data were collected with SMART 5.628 and were integrated with the SAINT<sup>2</sup> program. An empirical absorption correction was applied to collect reflections with SADABS<sup>3</sup> using XPREP<sup>4</sup>. The structure was solved using SIR-97<sup>5</sup> and refined using SHELXL-97<sup>6</sup>. The space group of the compounds was determined based on the lack of systematic absence and intensity statistics. Full matrix least squares / difference Fourier cycles were performed which located the remaining non-hydrogen atoms. All non-hydrogen atoms were refined with anisotropic displacement parameters. All the hydrogen atoms are fixed by using geometrical constraints using idealized geometries and have been defined isotropically.

**Table 1.** X-ray crystallographic data and structure refinement

Compounds	2a	2b
<b>Formula</b>	C <sub>18</sub> H <sub>19</sub> NO <sub>4</sub> S	C <sub>15</sub> H <sub>21</sub> NO <sub>4</sub> S
<b>Formula Weight</b>	345.40	311.39
<b>Crystal System</b>	monoclinic	monoclinic
<b>Space Group</b>	<i>P</i> 2 <sub>1</sub>	<i>P</i> 2 <sub>1</sub>
<b>Z</b>	2	2
<b>a, Å</b>	6.2717(16)	8.0088(16)
<b>b, Å</b>	17.050(4)	6.2986(13)
<b>c, Å</b>	8.096(2)	15.589(3)
<b>α, deg</b>	90.00	90.00
<b>β, deg</b>	103.844(4)	90.284(4)
<b>γ, deg</b>	90.00	90.00
<b>V, Å<sup>3</sup></b>	840.6(4)	786.4(3)
<b>d<sub>calcd.</sub>, g/cm<sup>3</sup></b>	1.365	1.315
<b>μ, mm<sup>-1</sup></b>	0.214	0.221
<b>F(000)</b>	364	332
<b>Refl. collected</b>	5341	3983
<b>Independent refl.</b>	3094	2581
<b>Refl. Observed [I &gt; 2σ (I)]</b>	2527	2453
<b>GOOF (F<sup>2</sup>)</b>	1.085	1.106
<b>R<sub>int</sub></b>	0.0494	0.0270
<b>Final R indices</b>	0.0484	0.0546
<b>[I &gt; 2σ(I)]<sup>[a]</sup></b>	0.0963	0.1391
<b>R indices (all data)<sup>[a]</sup></b>	0.0688	0.0575
	0.1180	0.1417

---

<sup>[a]</sup>Mo Kα radiation, <sup>b</sup>R<sub>1</sub> =  $\sum \|F_o\| - \|F_c\| / \sum \|F_o\|$ , <sup>c</sup>wR<sub>2</sub> =  $\{\sum [w(F_o^2 - F_c^2)^2] / \sum [w(F_o^2)^2]\}^{1/2}$

## 6. References

1. Perrin, D. D.; Armarego, W. L. F. Purification of Laboratory Chemicals; Third Edition; Pergamon Press: Oxford, 1988.
2. SAINT+ 6.02ed.; Bruker AXS, Madison, WI, **1999**.
3. Sheldrick, G. M. SADABS, Empirical Absorption Correction Program, University of Göttingen, Göttingen, Germany, **1997**.
4. XPREP, 5.1ed. Siemens Industrial Automation Inc., Madison, WI, **1995**.
5. Altomare, A.; Burla, M. C.; Camalli, M.; Cascarano, G. L.; Giacovazzo, C.; Guagliardi, A.; Moliterni, A. G. G.; Polidori, G.; Spagna, R. *J. Appl. Cryst.* **1999**, 32, 115.
6. Sheldrick, G. M. SHELXL-97: Program for Crystal Structure Refinement (University of Göttingen, Göttingen, Germany, **1997**).